Analysis of the Uplink Maximum Achievable Rate with Location Dependent Inter-cell Signal Interference Factors Based on Linear Wyner Model

Jing Zhang, *Member, IEEE,* Xiaohu Ge, *Senior Member, IEEE,* Zipeng Li, Guoqiang Mao, *Senior Member, IEEE,* and Yang Yang *Senior Member, IEEE*

***Abstract*—To enhance spectral efficiency, full frequency reuse has been adopted in advanced cellular communication networks, which however generates severe inter-cell co-channel interference and degrades the achievable rate at mobile terminals, especially for those located near cell boundaries. Therefore, it is of great importance and interests for network operators and service providers to evaluate and understand the impact of location dependent inter-cell co-channel interference on the achievable data rate in cellular networks. In this paper, considering a realistic spatial distribution of user locations, we first derive and analyze the probability density function (PDF) of the inter-cell power interference factor, which represents path loss of the adjacent cell signals, for the classic linear Wyner model. The closed form result of the maximum achievable rate in cellular uplink channels is also derived under the Nakagami-m fading model. Based on these new results, an upper bound of the uplink maximum achievable rate with location dependent inter-cell signal interference factors is calculated. Furthermore, the rate is analyzed in a running train scenario for the application of linear Wyner model. Numerical results show that user locations have strong impact on the maximum achievable rate per cell.**

I. INTRODUCTION

TO enhance the overall spectral efficiency in cellular networks, most schemes employ full frequency re-use in each cell. As a penalty, full frequency re-use often results in severe co-channel interferences and causes a significant drop of data rate at the terminals, particularly at the cell edge [1], [2]. The co-channel interferences significantly degrade the quality of service experienced by users located near the cell boundary, even with the adoption of multiple-input multiple-output (MIMO) and orthogonal frequency division multiplexing (OFDM) techniques [3], [4]. Therefore it is important to evaluate the impact of co-channel interference on the achievable rate of cellular networks.

Numerous single cell processing techniques have been proposed in the literature for improving the uplink capacity in wireless communication systems [5]–[8]. In [5], Liang et al. investigated the effect of various intra-cell schemes on uplink coverage spectral efficiency considering both single BS detection and joint adjacent BS detection. Furthermore, they analyzed the effect of adaptive channel reuse under different propagation models in the downlink channel of a one-dimensional linear cellular array considering only single BS transmission [6]. In [7], the accuracy of the Wyner model was studied in both uplink and downlink transmissions and considering both single-cell processing and multi-cell processing. In [8], Bang et al. investigated the gains of multicell zero-forcing beamforming (ZFBF) on the downlink of a Wyner-type network and compared the gap in data rate between ZFBF and single-cell processing (SCP) under mulituser scheduling. To overcome the interference problem in cellular networks, cooperative communication techniques have been proposed to combat the interference through the use of joint encoding and decoding at transmitters and receivers respectively. Some early studies investigating the uplink capacity of cooperative base stations (BSs) appeared in [9], [10]. Particularly in [9], considering high signal-to-noise ratio (SNR) wireless channels, Hanly et al. showed that by employing full frequency re-use, a larger capacity can be achieved in cellular networks compared with that using partial frequency re-use only and interference can be mitigated via the cooperation of BSs. In [10, pp. 1403], Wyner proposed a linear array cells model, i.e., the Wyner model, to analyze the capacity of cellular networks and defined the concept of inter-cell signal interference factor, which represents the path loss of the signals from the adjacent cells, to evaluate the impact of interference on the

Manuscript received December 4, 2011; revised May 22, 2012 and October 7, 2012; accepted November 2, 2012. The associate editor coordinating the review of this paper and approving it for publication was Dr. F. Richard Yu.

J. Zhang, X. Ge and Z. Li are with the Department of Electronics and Information Engineering, Huazhong University of Science and Technology, Wuhan 430074, Hubei, China (email: {zhangjing, xhge}@mail.hust.edu.cn, zipengli91@126.com).

G. Mao is with the School of Electrical and Information Engineering, University of Sydney and National ICT Australia, Sydney, Australia (email: guoqiang.mao@sydney.edu.au).

Y. Yang (corresponding author) is with the Shanghai Research Center for Wireless Communications (WiCO),Shanghai Institute of Microsystem and Information Technology,Chinese Academy of Sciences, Shanghai 200335, China (email: yang.yang@shrcwc.org).

The authors would like to acknowledge the support from the National Natural Science Foundation of China (NSFC) under the grants 60872007, 60902041 and 61271224, NFSC Major International Joint Research Project under the grant 61210002, National 863 High Technology Program of China under the grant 2009AA01Z239 and the Ministry of Science and Technology (MOST) of China under the grants 0903 and 2009DFB13080, the Hubei Provincial Science and Technology Department under the grant 2011BFA004 and the Fundamental Research Funds for the Central Universities under the grant 2011QN020. This research is partially supported by the National Natural Science Foundation of China (NSFC) under grant 61231009, the Science and Technology Commission of Shanghai Municipality (STCSM) under grant 11JC1412300 and RCUK for the UK-China Science Bridges Project: R&D on (B)4G Wireless Mobile Communications (EP/G042713/1), EU FP7-PEOPLE-IRSES, project acronym S2EuNet, contract/grant number: 247083. G. Mao would like to acknowledge the support from ARC Discovery DP110100538 and DP120102030.

uplink capacity of cellular networks. In [11], considering the co-channel interference and wireless channel fading, Shamai et al. used the maximum achievable rate per cell as a metric to evaluate the uplink capacity of cellular networks employing time division multiple access (TDMA), wideband (WB) and fractional intercell time-sharing (ICTS) schemes, respectively. Furthermore, in [12] and [13], a Gaussian soft-handoff model was presented to investigate the cooperative communication capacity of two cells. More specifically, in [12] the authors derived analytical expressions for the sum-rate capacities of uplink and downlink channels in cellular networks employing TDMA and WB schemes respectively. In [13] the benefit of BS cooperation for downlink transmission rates was investigated for cellular networks using dirty-paper-coding (DPC), zeroforcing (ZF) and minimum mean square error (MMSE) schemes, respectively. In [14]–[16], the authors studied the transmission rates assuming the Rayleigh wireless fading channels. Particularly, in [14], the Wyner model of cellular networks was employed to study the limits of maximum achievable rate per transmitter and the optimal performance in TDMA cellular networks. In [15], by using random matrices to model multi-user communication channels, the fluctuation of the maximum achievable rate per cell was studied. In [16], by resorting to random Schrodinger operators, bounds on the maximum achievable rate per cell were derived.

In [17], Bacha et al. considered the use of BSs with multiple antennas and derived the uplink sum capacity per cell for cellular networks with flat fading channels. In [18], Sanderovich considered a backhaul cellular network with joint multi-cell processing, i.e., the cell sites are linked to the central joint processor via lossless links with finite capacity, and derived the maximum achievable rates for the flat fading uplink channels assuming the Wyner and soft-handoff models. In [19], Nazer developed an inherent algebraic structure of lattice codes for improving the capacity of backhaul constrained cellular networks with flat fading uplink channels. For the downlinks of cooperative cellular networks, the maximum achievable rates were explored in [20]–[23]. Particularly, a linear pre-processing and encoding scheme based on the DPC method was proposed and a maximum achievable rate was derived in [20] for cellular networks with flat fading downlink channels. In [21], a closed-form formula for the maximum achievable rates was obtained which helped to obtain analytical insight into the impact of limited backhaul on the downlink throughput. An analytical co-channel interference model is proposed and exact normalized downlink average capacity is derived in [22] for multicell MIMO cellular networks. In [23], under an overall power constraint, Somekh et al. proposed a suboptimal cooperative multi-cell zero-forcing beamforming (ZFBF) scheme and showed that the scheme is capable of asymptotically achieving the same sum-rate growth rate compared with an optimal scheme deploying joint multi-cell DPC when the number of users in a cell approaches infinity.

In the aforementioned cellular network capacity studies, only a simple user distribution, e.g., uniform or Poisson, was considered. The random motion of users is assumed to have no impact on the spatial distribution of users in a cell [24]. Further, the inter-cell signal interference factor was considered as a fixed constant when evaluating the maximum achievable rate in cellular networks and little work considered the impact of user locations in a cell on the inter-cell signal interference factor. Additionally, only the traditional Rayleigh fading channels were considered in the above work and the maximum achievable rate analysis under the more general Nakagami-m fading uplink channels has not been investigated.

Motivated by the above observations, in this paper we study the maximum achievable rate per cell for cellular networks with Nakagami-m fading uplink channels considering location dependent inter-cell signal interference factors. The contributions and novelties of this paper are summarized in the following.

1) The probability density function (PDF) of the inter-cell power interference factor for linear Wyner cells is derived, which is used to calibrate the interference from users considering the impact of their location distribution.
2) A closed-form expression for the maximum achievable rate per cell is derived for linear cellular networks with Nakagami-m fading uplink channels.
3) Based on a running train scenario, a new maximum achievable rate per cell is derived for linear cellular networks with Nakagami-m fading uplink channels considering location dependent inter-cell signal interference factors. Further, an upper bound of maximum achievable rate is also obtained.

The rest of paper is organized as follows. Section II describes the system model. In Section III, the PDF of the inter-cell power interference factor in linear Wyner cells is derived. Assuming Nakagami-m fading uplink channels, a closed-form expression for the maximum achievable rate per cell is derived in Section IV. In Section V, a maximum achievable rate per cell with location dependent inter-cell signal interference factors in a running train scenario is proposed and evaluated by numerical results. Finally, Section VI concludes this paper.

II. System Model

Consider a linear array of M cells with one BS and K users per cell. The radius of each cell is assumed to be R. Users are assumed to be independently and identically distributed (i.i.d.) in a cell following a uniform distribution. Further, it is assumed that users within the same cell use different channels to communicate and users belonging to different BSs may however use the same channel due to full spatial frequency reuse. In this case, the multi-user diversity effect in a cell will be analyzed in the following sections. Therefore, a BS receives the desired signal from users located within the same cell and interference is caused by users in adjacent cells. The above model is known as the linear Wyner model [10] and is illustrated in Fig.1.

The signals received by the M BSs may be represented in a vector form as follows:

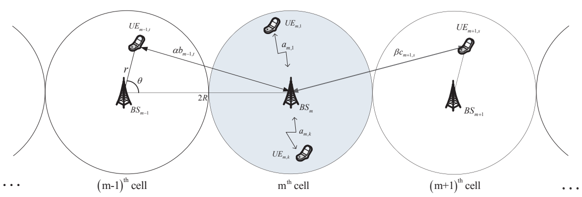

Fig. 1. A general linear Wyner model.

$$\vec{y} = H\vec{x} + \vec{n}, \tag{1}$$

where $\vec{y}$ is a $M \times 1$ column vector representing signals received by the M BSs, $\vec{x}$ is a $MK \times 1$ column vector representing uplink signals sent by K users, H is a $M \times MK$ channel transfer matrix and $\vec{n}$ is a $M \times 1$ column vector denoting the noise received by the M BSs.

Based on the traditional Wyner model, BS_m, i.e., the base station in the m^{th} cell, $m \in [1, M]$, only receives co-channel interference from users in adjacent cells, i.e., the $(m-1)^{th}$ cell and the $(m+1)^{th}$ cell, and the interference from users in other cells is assumed to be negligible (see Fig. 1). Denote by $UE_{m,k}$, $m \in [1, M]$ and $k \in [1, K]$, the k^{th} active user in the m^{th} cell and denote by $UE_{m-1,t}$, $UE_{m+1,s}$, $t \in [1, K]$ and $s \in [1, K]$, the t^{th} interfering user in the $(m-1)^{th}$ cell and the s^{th} interfering user in the $(m+1)^{th}$ cell, respectively. The channel transfer matrix H in (1) can then be written as

$$H = \begin{pmatrix} \vec{a}_1 & \beta\vec{c}_2 & 0 & \cdots & 0 & 0 \\ \alpha\vec{b}_1 & \vec{a}_2 & \beta\vec{c}_3 & 0 & \cdots & 0 \\ 0 & \alpha\vec{b}_2 & \vec{a}_3 & \beta\vec{c}_4 & \ddots & \vdots \\ \vdots & 0 & \alpha\vec{b}_3 & \ddots & \ddots & 0 \\ 0 & \vdots & \ddots & \ddots & \vec{a}_{M-1} & \beta\vec{c}_M \\ 0 & 0 & \cdots & 0 & \alpha\vec{b}_{M-1} & \vec{a}_M \end{pmatrix}, \tag{2}$$

where $\vec{a}_m = [a_{m,1}, a_{m,2}, \cdots, a_{m,k}, \cdots, a_{m,K}]$, $m \in [1, M]$ and $k \in [1, K]$, is a $1 \times K$ random vector, representing the multi-path and shadow fading effect experienced by the desired signals from K active users in the m^{th} cell, $\vec{b}_{m-1} = [b_{m-1,1}, b_{m-1,2}, \cdots, b_{m-1,t}, \cdots, b_{m-1,K}]$ and $\vec{c}_{m+1} = [c_{m+1,1}, c_{m+1,2}, \cdots, c_{m+1,s}, \cdots, c_{m+1,K}]$, t and $s \in [1, K]$, are two $1 \times K$ random vectors representing the multi-path and shadow fading effect experienced by the interference signals from users in the $(m-1)^{th}$ and $(m+1)^{th}$ cells, respectively. It is assumed that $a_{m,k}$, $b_{m-1,t}$ and $c_{m+1,s}$, are random complex variables, and are statistically independent of each other.

The parameter $\alpha \in [0, 1]$ is the *inter-cell signal interference factor*, which represents the path loss of interfering signals from users in the $(m-1)^{th}$ cell to the m^{th} cell [14]. Considering that the interference signals are statistically independent, the inter-cell signal interference factor from users in the $(m+1)^{th}$ cell to the m^{th} cell is $\beta \in [0, 1]$. As commonly done in the area, it is assumed that the nodes mobility is such that the spatial distribution of nodes location is stationary and ergodic with stationary distribution uniform in its cell [14], [25]. It follows that the inter-cell signal interference factors α and β can be approximated by its spatial average value [24], i.e., the average inter-cell signal interference factor, and be treated as a constant in cellular networks. In the next section, we will show how to obtain the values of α and β considering the spatial random distribution of interfering users' location in a cell.

Considering the impact of interference and noise in the linear Wyner model, the maximum achievable rate with single cell processing scheme R_{SCP_m} in the m^{th} cell is given by [10]

$$R_{SCP\_m} = E\left\{\log\left(1 + \frac{P_m}{N_m + I_m}\right)\right\}, \tag{3}$$

where P_m is the instantaneous received signal power at BS, I_m is the instantaneous interference power from the $(m-1)^{th}$ and $(m+1)^{th}$ cell, N_m is the instantaneous noise power, $E\{\cdot\}$ is an expectation operator which takes over instantaneous signal power, interference power and noise power to get the average data rate. To avoid the near-far effect in cellular networks, the user terminals generally adaptively adjust the transmission power to keep all signal power received by BSs at the same level. Therefore, the received power at the BS is represented by a common value. Based on the simple one-slope path loss model, the instantaneous received power at BS BS_m is traditionally expressed as

$$P_m = \frac{\Re \bar{P}_{tr}}{K} \sum_{k=1}^{K} (d_0/d_{m,k})^{\lambda} |a_{m,k}|^2, \tag{4}$$

where $\bar{P}_{tr}$ is the transmission power of users in a cell, $d_{m,k}$ is a distance between the transmitter and the receiver, d_0 is a reference distance and $\bar{P}_{tr}$ is the received power at d_0, λ is an attenuation coefficient and $\Re$ is an propagation coefficient, $\Re = -31.54dB$ when $d_0 = 1$ meter [26]. The instantaneous interference power from users in the $(m-1)^{th}$ and $(m+1)^{th}$ cells to the BS in the m^{th} cell can be written as (5), where $d_{m-1,t}$ and $d_{m+1,s}$ are the distances between the transmitters and the receivers with the same channels in the $(m-1)^{th}$ and $(m+1)^{th}$ cells, and the BS in the m^{th} cell, $t, s \in [1, K]$ are the indices of users in the $(m-1)^{th}$ and $(m+1)^{th}$ cells, respectively.

The noise is assumed as a zero mean, i.i.d. Gaussian process. For the sake of simplicity, the noise power in uplink channel is normalized to a unit power in this paper. Then, substituting (3) by the instantaneous received power, interference power and noise power, the R_{SCP_m} can be rewritten as (6).

Define the inter-cell average power interference factor as $\overline{\alpha^2} = \sum\limits_{t=1}^{K} {d_{m-1,t}}^{-\lambda} \Big/ \sum\limits_{k=1}^{K} {d_{m,k}}^{-\lambda}$, $\overline{\beta^2} = \sum\limits_{s=1}^{K} {d_{m+1,s}}^{-\lambda} \Big/ \sum\limits_{k=1}^{K} {d_{m,k}}^{-\lambda}$ and replace the average user data rates in (6) with the approximated rates derived from [27], the R_{SCP_m} is approximated as (7), where $a_{m,k}$,

$$I_m = \frac{\Re \bar{P}_{tr}}{K}\left(\sum_{t=1}^{K}(d_0/d_{m-1,t})^{\lambda}|b_{m-1,t}|^2 + \sum_{s=1}^{K}(d_0/d_{m+1,s})^{\lambda}|c_{m+1,s}|^2\right). \tag{5}$$

$$\begin{aligned}
R_{SCP_m} &= E\left\{\log\left(1+\frac{\frac{\Re\bar{P}_{tr}}{K}\sum\limits_{k=1}^{K}\left(\frac{d_0}{d_{m,k}}\right)^{\lambda}|a_{m,k}|^2}{1+\frac{\Re\bar{P}_{tr}}{K}\left(\sum\limits_{t=1}^{K}\left(\frac{d_0}{d_{m-1,t}}\right)^{\lambda}|b_{m-1,t}|^2+\sum\limits_{s=1}^{K}\left(\frac{d_0}{d_{m+1,s}}\right)^{\lambda}|c_{m+1,s}|^2\right)}\right)\right\}\\
&= E\left\{\log\left(1+\frac{\frac{\bar{P}_{tr}}{K}\sum\limits_{k=1}^{K}{d_{m,k}}^{-\lambda}|a_{m,k}|^2}{\frac{1}{\Re\sum\limits_{k=1}^{K}d_0^{\lambda}}+\frac{\bar{P}_{tr}}{K}\left(\sum\limits_{t=1}^{K}{d_{m-1,t}}^{-\lambda}|b_{m-1,t}|^2+\sum\limits_{s=1}^{K}{d_{m+1,s}}^{-\lambda}|c_{m+1,s}|^2\right)}\right)\right\}\\
&= E\left\{\log\left(1+\frac{\frac{\bar{P}_{tr}}{K}\sum\limits_{k=1}^{K}|a_{m,k}|^2}{\frac{1}{\Re\sum\limits_{k=1}^{K}\left(\frac{d_0}{d_{m,k}}\right)^{\lambda}}+\frac{\bar{P}_{tr}}{K}\left(\frac{\sum\limits_{t=1}^{K}{d_{m-1,t}}^{-\lambda}}{\sum\limits_{k=1}^{K}{d_{m,k}}^{-\lambda}}\sum\limits_{t=1}^{K}|b_{m-1,t}|^2+\frac{\sum\limits_{s=1}^{K}{d_{m+1,s}}^{-\lambda}}{\sum\limits_{k=1}^{K}{d_{m,k}}^{-\lambda}}\sum\limits_{s=1}^{K}|c_{m+1,s}|^2\right)}\right)\right\}
\end{aligned}, \tag{6}$$

$$R_{SCP\_m} \approx E\left\{\log\left(1+\frac{\frac{\bar{P}_{tr}}{K}\sum\limits_{k=1}^{K}|a_{m,k}|^2}{1+\frac{\bar{P}_{tr}}{K}\left(\overline{\alpha^2}\sum\limits_{t=1}^{K}|b_{m-1,t}|^2+\overline{\beta^2}\sum\limits_{s=1}^{K}|c_{m+1,s}|^2\right)}\right)\right\}, \tag{7}$$

$b_{m-1,t}$ and $c_{m+1,s}$ are the channel propagation coefficients of the m^{th}, $(m-1)^{th}$ and $(m+1)^{th}$ cell respectively.

The above equation is obtained assuming that users move randomly in a cell. However, in some applications, for example when all interfering users are seated in a running train, the user's mobility model is no longer random but rather predictable. In these situations, the inter-cell power interference factor is obviously significantly affected by the user's location in a cell, and can no longer be approximated by an average value. Further, it is interesting to evaluate the impact of the user location-dependent inter-cell power interference factor on the maximum achievable rate of cellular networks and derive a closed-form solution. Besides, it can be seen from (7) that the maximum-achievable rate is affected by the interference factor and the channel propagation coefficient, i.e., the slow lognormal shadowing and fast multipath fading. Considering the path loss is independent on the slow lognormal shadowing and fast multipath fading in wireless channels [26], the PDF of inter-cell interference factor is first derived to evaluate the impact of user's location on the maximum-achievable rate in cellular networks. Furthermore, the impact of the slow lognormal shadowing and fast multipath fading modelled by the Nakagami-m fading on the maximum achievable rate of cellular networks is studied in Section IV. Finally, we will analyze the interference factor and Nakagami-m fading for the maximum achievable rate in a running train scenario using a linear Wyner model.

Besides, it can be seen from (7) that the maximum-achievable rate is affected by the interference factor and the channel propagation coefficient, i.e., the slow lognormal shadowing and fast multipath fading. Considering the path loss is independent on the slow lognormal shadowing and fast multipath fading in wireless channels [26], the PDF of inter-cell interference factor is first derived to evaluate the impact of user's location on the maximum-achievable rate in cellular networks. Furthermore, the impact of the slow lognormal shadowing and fast multipath fading modelled by the Nakagami-m fading on the maximum achievable rate of cellular networks is studied in Section IV. Finally, we will analyze the interference factor and Nakagami-m fading for the maximum achievable rate in a running train scenario using a linear Wyner model.

III. PDF OF INTER-CELL POWER INTERFERENCE FACTOR

To derive a closed-form expression of the maximum achievable rate considering location dependent inter-cell signal interference factors, the PDF of inter-cell power interference factor is firstly investigated in this section.

Considering that the interference occurs when the users in different cells are allocated the same channel, the same code in CDMA system or the same frequence in OFDM system, the inter-cell average power interference factor of one user is analyzed. The inter-cell power interference factor of one user will be discussed firstly. As illustrated in Fig. 1, let r be the distance between $UE_{m-1,k}$ and BS_{m-1} and let

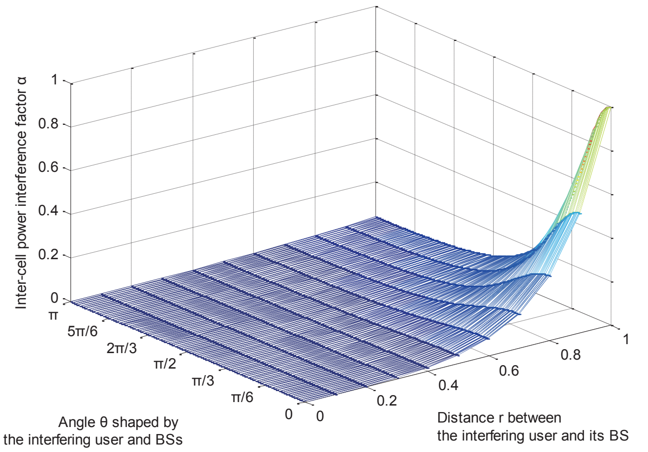

Fig. 2. Inter-cell power interference factor with respect to the user location.

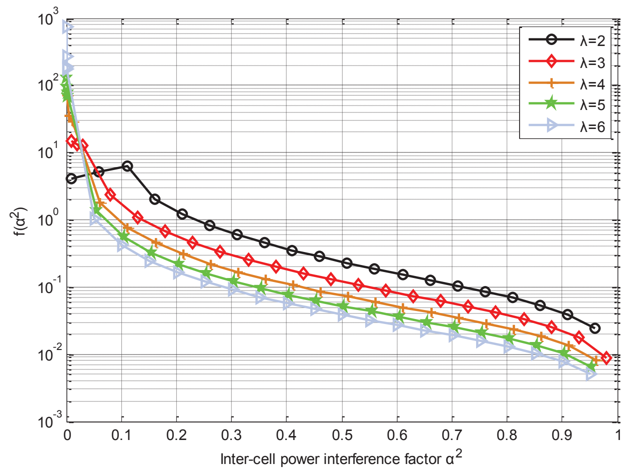

Fig. 3. PDF of inter-cell power interference factor.

the angle subtended by $UE_{m-1,k}$, BS_{m-1} and BS_m be θ. Using the definition of inter-cell signal interference factor, the inter-cell power interference factor α^2 of $UE_{m-1,k}$ is derived by (8) [18].

Fig. 2 plots the inter-cell power interference factor as a function of the user location parameters θ and r for the situation of a fixed attenuation coefficient $\lambda = 2$ using (8). As shown in Fig. 2, the inter-cell power interference factor is a monotonically increasing function of the distance r and is a monotonically decreasing function of the angle θ. Moreover, the maximum of inter-cell power interference factor is reached when the interfering user is located at the cell-edge with $r = R$ and $\theta = 0$.

To facilitate the derivation of the PDF of the inter-cell power interference factor, an intermediate variable $\mathcal{G} = \frac{r}{\sqrt{(r\cos\theta - 2R)^2 + r^2\sin^2\theta}}$ is defined. Moreover, considering that users are assumed to follow a uniform distribution in a cell, the cumulative distribution function (CDF) of $\mathcal{G}$ is given by (9) [28].

Based on the result of Appendix, the CDF of $\mathcal{G}$ can be further written as (10) [29].

As a consequence, the PDF of $\mathcal{G}$ is derived by derivative as (11).

Considering the relationship of $\alpha^2 = \mathcal{G}^\lambda$, the PDF of inter-cell power interference factor α^2 is finally derived by following segmented functions: when $0 \le \alpha^{\frac{2}{\lambda}} \le \frac{1}{3}$, the PDF of α^2 is derived as (12a), when $\frac{1}{3} < \alpha^{\frac{2}{\lambda}} \le 1$, the PDF of α^2 is derived as (12b).

The PDF of the inter-cell power interference factor with respect to the attenuation coefficient λ is illustrated in Fig. 3. Considering an urban macrocell environment, the attenuation coefficient λ is ranged from 2 to 5 [30]. To clearly compare the numerical results, the logarithm curves of the PDF of the inter-cell power interference factor are plotted in Fig. 3. From Fig. 3, it can be seen there is a maximum peak value of PDF curve with $\lambda = 2$. The reason caused this result is that (12a) is a monotone increasing function of α^2 and (12b) is a monotone decreasing function of α^2 when the attenuation coefficient is equal to 2. Therefore, there must exist a maximum peak value when $\left(\alpha^2\right)^{\frac{1}{2}} = 1/3$, i.e., $\alpha^2 = 1/9$. However, when the attenuation coefficient λ is large than or equal to 3, (12a) and (12b) are all monotone decreasing function of α^2. In this case, the maximum peak value of $f\left(\alpha^2\right)$ is occurred when $\alpha^2 = 0$.

IV. Maximum Achievable Rate with Nakagami-m Fading Uplink Channels and Fixed Interference Factors

In this section, the impact of channel propagation coefficient modelled by the Nakagami-m fading on the maximum-achievable rate is evaluated. Considering that the path loss is independent on the Nakagami-m fading, the inter-cell interference factor is fixed. Furthermore, a closed-form expression of the maximum achievable rate per cell over Nakagami-m fading uplink channels is derived based on Meijer G-functions.

To facilitate the derivation of the maximum achievable rate, three random variables are defined: $S = \sum_{k=1}^{K} |a_{m,k}|^2$, $T_L = \sum_{t=1}^{K} |b_{m-1,t}|^2$ and $T_R = \sum_{t=1}^{K} |c_{m+1,s}|^2$. The maximum achievable rate in (7) can be written in the form of the three random variables as (13). Considered the inter-cell power interference factor is dependant on the location of user, $\overline{\alpha^2}$ and $\overline{\beta^2}$ are the average inter-cell power interference factors from the $(m-1)^{th}$ and $(m+1)^{th}$ cells.

In the system model illustrated in Fig. 1, the general Nakagami-m fading uplink channels are considered. Moreover, every signal including the interference signal is assumed to be independent and is subject to independent Nakagami-m fading. In this case, the PDF of Z, which represents the signal envelope in wireless uplink channels, is expressed by a Nakagami-m distribution [31]

$$\alpha^2 = \frac{\bar{P}_{tr}\mathfrak{K}\left(d_0 \Big/ \sqrt{(r\cos\theta - 2R)^2 + r^2\sin^2\theta}\right)^\lambda}{\bar{P}_{tr}\mathfrak{K}(d_0/r)^\lambda} = \left(\frac{r}{\sqrt{(r\cos\theta - 2R)^2 + r^2\sin^2\theta}}\right)^\lambda. \tag{8}$$

$$F_{\mathcal{G}}(\gamma) = \iint\limits_{\frac{r}{\sqrt{(r\cos\theta-2R)^2+r^2\sin^2\theta}} \leqslant \gamma} f(r,\theta)\, dS = \iint\limits_{\frac{r}{\sqrt{(r\cos\theta-2R)^2+r^2\sin^2\theta}} \leqslant \gamma} \frac{r}{\pi R^2} dr d\theta. \tag{9}$$

$$\begin{aligned} &F_{\mathcal{G}}(\gamma) \\ &= \begin{cases} \frac{4\gamma^2}{(\gamma^2-1)^2} & 0 \le \gamma \le \frac{1}{3} \\ 1 - \frac{(\gamma^2+1)^2 \arccos\frac{5\gamma^2-1}{4\gamma^2}}{\pi(\gamma^2-1)^2} - \frac{\sqrt{(9\gamma^2-1)}(1-\gamma^2)^{-\frac{1}{2}}}{2\pi} - \frac{4\gamma^2}{\pi(\gamma^2-1)^2}\arcsin\frac{\sqrt{(1-9\gamma^2)(\gamma^2-1)}}{4\gamma} & \frac{1}{3} < \gamma \le 1 \end{cases} \end{aligned}. \tag{10}$$

$$\begin{aligned} &f_{\mathcal{G}}(\gamma) \\ &= \begin{cases} \frac{-8\gamma(\gamma^2+1)}{(\gamma^2-1)^3} & 0 \le \gamma \le \frac{1}{3} \\ -\frac{8\gamma(\gamma^2+1)}{\pi(\gamma^2-1)^3}\left(\arccos\frac{5\gamma^2-1}{4\gamma^2} - \arcsin\frac{\sqrt{(1-9\gamma^2)(\gamma^2-1)}}{4\gamma}\right) - \frac{2(9\gamma^2-1)^{\frac{1}{2}}}{\pi\gamma(1-\gamma^2)^{\frac{3}{2}}} & \frac{1}{3} < \gamma \le 1 \end{cases} \end{aligned}. \tag{11}$$

$$f\left(\alpha^2\right) = \frac{-8\alpha^{2\frac{1}{\lambda}}\left(\alpha^{2\frac{2}{\lambda}}+1\right)}{\left(\alpha^{2\frac{2}{\lambda}}-1\right)^3}\frac{1}{\lambda}\alpha^{2\left(\frac{1}{\lambda}-1\right)}, \tag{12a}$$

$$\begin{aligned} f\left(\alpha^2\right) = &-\frac{8\alpha^{2\frac{1}{\lambda}}\left(\alpha^{2\frac{2}{\lambda}}+1\right)}{\pi\left(\alpha^{2\frac{2}{\lambda}}-1\right)^3}\frac{1}{\lambda}\alpha^{2\left(\frac{1}{\lambda}-1\right)}\left(\arccos\frac{5\alpha^{2\frac{2}{\lambda}}-1}{4\alpha^{2\frac{2}{\lambda}}} - \arcsin\frac{\sqrt{\left(1-9\alpha^{2\frac{2}{\lambda}}\right)\left(\alpha^{2\frac{2}{\lambda}}-1\right)}}{4\alpha^{2\frac{1}{\lambda}}}\right) \\ &-\frac{2\left(9\alpha^{2\frac{2}{\lambda}}-1\right)^{\frac{1}{2}}}{\pi\alpha^{2\frac{1}{\lambda}}\left(1-\alpha^{2\frac{2}{\lambda}}\right)^{\frac{3}{2}}}\frac{1}{\lambda}\alpha^{2\left(\frac{1}{\lambda}-1\right)} \end{aligned}. \tag{12b}$$

$$\begin{aligned} R_{SCP\_m} &= E\left\{\log\left(1 + \frac{\bar{P}_{tr}\sum_{k=1}^{K}|a_{m,k}|^2}{K+\overline{\alpha^2}\bar{P}_{tr}\sum_{t=1}^{K}|b_{m-1,t}|^2+\overline{\beta^2}\bar{P}_{tr}\sum_{t=1}^{K}|c_{m+1,s}|^2}\right)\right\} \\ &= E\left\{\log\left(1 + \frac{\bar{P}_{tr}S}{K+\bar{P}_{tr}\overline{\alpha^2}T_L+\bar{P}_{tr}\overline{\beta^2}T_R}\right)\right\} \\ &= E\left\{\log\left(K + \bar{P}_{tr}\left(S + \overline{\alpha^2}T_L + \overline{\beta^2}T_R\right)\right) - \log\left(K + \bar{P}_{tr}\left(\overline{\alpha^2}T_L + \overline{\beta^2}T_R\right)\right)\right\} \end{aligned}, \tag{13}$$

$$f_Z(x) = \frac{2\left(\frac{m_l}{\Omega}\right)^{m_l}}{\Gamma(m_l)}x^{2m_l-1}e^{\left(-\frac{m_l x^2}{\Omega}\right)}, \tag{14}$$

where m_l is a fading severity parameter, Ω is a received signal power at the corresponding BS. Furthermore, the PDF of Z^2 can be approximated by a Gamma distribution [32]

$$f_{Z^2}(x) = \frac{\left(\frac{m_l}{\Omega}\right)^{m_l}}{\Gamma(m_l)}x^{m_l-1}e^{\left(-\frac{m_l x}{\Omega}\right)}, \tag{15}$$

which can be simply denoted as $Z^2 \sim \Gamma(m_l, \Omega/m_l)$.

Using (15), the Nakagami-m fading effect of desired signal in the m^{th} cell and interference signal in the $(m-1)^{th}$ and $(m+1)^{th}$ cells, represented by $|a_{m,k}|^2$, $|b_{m-1,t}|^2$ and $|c_{m+1,s}|^2$ can be expressed by Gamma distributions: $|a_{m,k}|^2 \sim \Gamma(m_1, \Omega/m_1)$, $|b_{m-1,t}|^2 \sim \Gamma(m_2, \Omega/m_2)$, and $|c_{m+1,s}|^2 \sim \Gamma(m_3, \Omega/m_3)$, respectively. Parameters m_1, m_2 and m_3 are fading severity parameters in the m^{th}, $(m-1)^{th}$ and $(m+1)^{th}$ cells respectively.

Moreover, two important lemmas used for derivation are listed as follows [33]:

Lemma 1: Let $X_{i=1,2,\ldots\mathrm{N}}$ be a set of independent random variables and $X_i \sim \Gamma(a_{\Gamma,i}, b_\Gamma)$(i.e., all distributions have the same scale parameter b_Γ), then $\sum_{i=1}^{N} X_i \sim \Gamma\left(\sum_{i=1}^{N} a_{\Gamma,i}, b_\Gamma\right)$.

Lemma 2: Let $X \sim \Gamma(a_\Gamma, b_\Gamma)$, then for any $k > 0$, $kX \sim \Gamma(a_\Gamma, kb_\Gamma)$.

The Nakagami-m fading effect on the desired signal in the m^{th} cell and interference signals in the $(m-1)^{th}$ cell, i.e., $|a_{m,k}|^2$ and $|b_{m-1,t}|^2$ are assumed independent. The Nakagami-m fading severity parameters are assumed same for all users in a cell. The distributions of random variables S, $\overline{\alpha^2}T_L$ and $\overline{\beta^2}T_R$ can be obtained as (16), (17) and (18).

According to the conditions in [34], the PDF of the sum of two independent Gamma variables i.e., $\overline{\alpha^2}T_L + \overline{\beta^2}T_R$, is given by (19), where ${}_1F_1(a_F, b_F; c_F) = 1 + \frac{a_F}{b_F}\frac{c_F}{1!} + \frac{a_F(a_F+1)}{b_F(b_F+1)}\frac{{c_F}^2}{2!} + \cdots$, is a confluent hypergeometric function and is defined in [35, pp. 1023].

In [36], the exact PDF of the sum of three Gamma random variables, i.e., $S + \overline{\alpha^2}T_L + \overline{\beta^2}T_R$, can be expressed as (20), where $\Delta = m_1^{Km_1}\left(\frac{\overline{\beta^2}}{m_3}\right)^{Km_1+Km_2}\left(\frac{m_2}{\overline{\alpha^2}}\right)^{Km_2}$, $\rho = K(m_1+m_2+m_3)$, δ_i is found by recursion from $\delta_{i+1} = \frac{1}{i+1}\sum_{j=1}^{i+1} j\gamma_j\delta_{i+1-j}$, and $\gamma_j = j^{-1}\Omega\left[\frac{1}{m_1}\left(1-\frac{\overline{\beta^2}m_1}{m_3}\right)^j + \frac{\overline{\alpha^2}}{m_2}\left(1-\frac{\overline{\beta^2}m_2}{\overline{\alpha^2}m_3}\right)^j\right]$.

However, the closed-form PDF is difficult to be derived from the expression in (20). To derive a closed-form PDF for the sum of three independent Gamma random variables that can be readily computed, a moment matching approximation approach with the same first and second order moments is used for (20). The gamma distributed variable V with the same first and second order moments equals to those of $S + \overline{\alpha^2}T_L + \overline{\beta^2}T_R$ is given by [37]

$$V \sim \Gamma(\kappa, \Theta) = \frac{y^{\kappa-1}e^{-\frac{y}{\Theta}}}{\Theta^\kappa \Gamma(\kappa)} \tag{21a}$$

with

$$\kappa = \frac{K\left(1+\overline{\alpha^2}+\overline{\beta^2}\right)^2}{\left(\frac{1}{m_1}+\frac{\overline{\alpha^4}}{m_2}+\frac{\overline{\beta^4}}{m_3}\right)}, \tag{21b}$$

$$\Theta = \frac{\Omega\left(\frac{1}{m_1}+\frac{\overline{\alpha^4}}{m_2}+\frac{\overline{\beta^4}}{m_3}\right)}{1+\overline{\alpha^2}+\overline{\beta^2}}. \tag{21c}$$

Substitute (19) and (21a) into (13), a new maximum achievable rate with Nakagami-m fading uplink channels is derived by (22a) with (22b), where ${}_1F_1(\cdot;\cdot;\cdot)$ is a confluent hypergeometric function.

The integral in (22a) is difficult to compute. To simplify the expression, we resort to some special functions, i.e., the so-called Meijer's G-functions, which is defined as (23) [38], where $0 \le m \le q$, $0 \le n \le p$, and $\Im = \sqrt{-1}$. The $\log_2(\cdot)$ and ${}_1F_1(\cdot;\cdot;\cdot)$ functions can be expressed as a special form of Meijer's G-function. Therefore, (22) can be expressed in a closed-form using Meijer's G-functions as (24a) with (24b).

A. Numerical Analysis of Maximum Achievable Rate with Nakagami-m Fading Uplink Channels

Based on the maximum achievable rate with Nakagami-m fading uplink channels obtained in the last section, some numerical performance evaluations are performed. The following parameters are used in the numerical evaluation: the received signal power Ω at a BS is normalized as 1, the average user transmission power is configured $\bar{P}_{tr} = 10$dB, the Nakagami-m fading severity parameter in the $(m-1)^{th}$ and $(m+1)^{th}$ cells are chosen to be $m_2 = 1$, $m_3 = 2$, respectively, and the signal interference factor from the $(m+1)^{th}$ cell is chosen to be $\beta = 0.3$.

Supposing that the number of users in a cell $K = 10$, in Fig. 4, the maximum achievable rate per cell for different channel conditions is shown. In Fig. 4, the maximum achievable rate per cell decreases with the increase of the inter-cell signal interference factor. When the inter-cell signal interference factor is fixed, the maximum achievable rate per cell increases with the increase of the Nakagami-m fading severity parameter m_1 in the m^{th} cell.

Given that the Nakagami-m fading severity parameter in the m^{th} cell is chosen to be $m_1 = 1$, Fig. 5 illustrates the maximum achievable rate per cell as a function of the number of users in a cell. When the inter-cell signal interference factor is less than 0.67, the maximum achievable

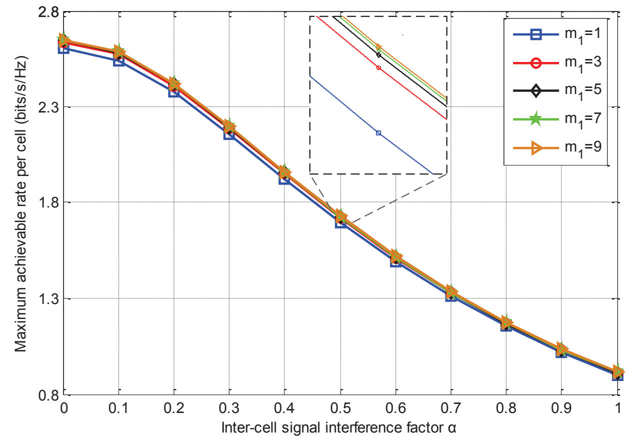

Fig. 4. Maximum achievable rate per cell with respect to the inter-cell signal interference factor and the signal fading severity parameter.

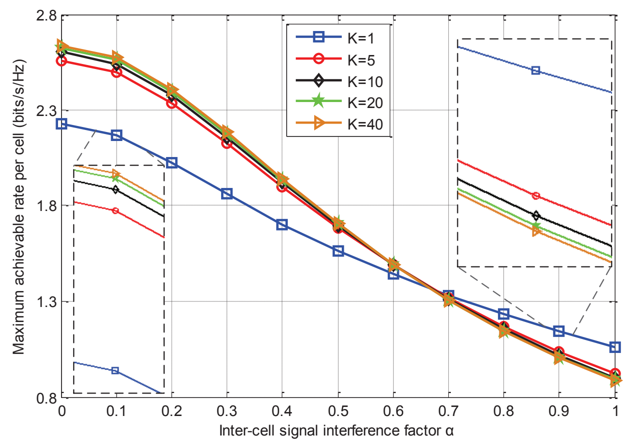

Fig. 5. Maximum achievable rate per cell with respect to the inter-cell signal interference factor and the user number in a cell.

$$S = \sum_{k=1}^{K} \left| a_{m,k} \right|^2 \sim \Gamma\left(Km_1, \Omega/m_1\right) = \frac{\left(\frac{m_1}{\Omega}\right)^{Km_1}}{\Gamma\left(Km_1\right)} x^{Km_1-1} e^{\left(-\frac{m_1 x}{\Omega}\right)}, \tag{16}$$

$$\overline{\alpha^2} T_L = \overline{\alpha^2} \sum_{k=1}^{K} \left| b_{m-1,t} \right|^2 \sim \Gamma\left(Km_2, \overline{\alpha^2}\Omega \big/ m_2\right) = \frac{\left(\frac{m_2}{\overline{\alpha^2}\Omega}\right)^{Km_2}}{\Gamma\left(Km_2\right)} x^{Km_2-1} e^{\left(-\frac{m_2 x}{\overline{\alpha^2}\Omega}\right)}, \tag{17}$$

$$\overline{\beta^2} T_R = \overline{\beta^2} \sum_{k=1}^{K} \left| c_{m+1,s} \right|^2 \sim \Gamma\left(Km_3, \overline{\beta^2}\Omega \big/ m_3\right) = \frac{\left(\frac{m_3}{\overline{\beta^2}\Omega}\right)^{Km_3}}{\Gamma\left(Km_3\right)} x^{Km_3-1} e^{\left(-\frac{m_3 x}{\overline{\beta^2}\Omega}\right)}. \tag{18}$$

$$f_{\overline{\alpha^2}T_L + \overline{\beta^2}T_R}\left(x\right) = \frac{x^{Km_2+Km_3-1} e^{-m_3 x/\overline{\beta^2}\Omega} {}_1F_1\left[Km_2; Km_2+Km_3; \left(\frac{m_3}{\overline{\beta^2}\Omega} - \frac{m_2}{\overline{\alpha^2}\Omega}\right)x\right]}{\left(\frac{\overline{\alpha^2}\Omega}{m_2}\right)^{Km_2} \left(\frac{\overline{\beta^2}\Omega}{m_3}\right)^{Km_3} \Gamma\left(Km_2+Km_3\right)}, \tag{19}$$

$$f_{S+\overline{\alpha^2}T_L+\overline{\beta^2}T_R}\left(y\right) = \Delta \sum_{i=0}^{\infty} \frac{\delta_i m_3^{\rho+i}}{\Gamma\left(\rho+i\right)\left(\overline{\beta^2}\Omega\right)^{\rho+i}} y^{\rho+i-1} e^{-xm_3/\overline{\beta^2}\Omega} \tag{20}$$

$$\begin{aligned} R_{SCP\_m} &= \int_0^\infty \log\left(K+\bar{P}_{tr}y\right) \tfrac{y^{\kappa-1} e^{-\frac{y}{\Theta}}}{\Theta^{\kappa}\Gamma(\kappa)} dy \\ &-\tfrac{1}{\varepsilon}\int_0^\infty \log\left(K+\bar{P}_{tr}x\right) x^{Km_2+Km_3-1} e^{-m_3 x/\overline{\beta^2}\Omega} {}_1F_1\left[Km_2; Km_2+Km_3; \left(\tfrac{m_3}{\overline{\beta^2}\Omega} - \tfrac{m_2}{\overline{\alpha^2}\Omega}\right)x\right] dx \end{aligned}, \tag{22a}$$

$$\varepsilon = \left(\frac{\overline{\alpha^2}\Omega}{m_2}\right)^{Km_2} \left(\frac{\overline{\beta^2}\Omega}{m_3}\right)^{Km_3} \Gamma\left(Km_2+Km_3\right). \tag{22b}$$

$$G_{p,q}^{m,n}\left(x \left| \begin{array}{c} a_1, \cdots a_p \\ b_1, \cdots b_q \end{array} \right.\right) = \frac{1}{2\pi\Im} \int_0^\infty \frac{\prod\limits_{j=1}^{m} \Gamma(b_j - s) \prod\limits_{j=1}^{n} \Gamma(1-a_j+s)}{\prod\limits_{j=m+1}^{q} \Gamma(1-b_j+s) \prod\limits_{j=n+1}^{p} \Gamma(a_j - s)} x^s ds, \tag{23}$$

$$\begin{aligned} R_{SCP\_m} &= \tfrac{1}{\Gamma(k)} G_{3,2}^{1,3}\left(\begin{array}{c} 1-k,1,1 \\ 1,0 \end{array} \left| \tfrac{\overline{P_{tr}}\Theta}{K} \right.\right) + \log K \\ &-\varepsilon_t \left(\tfrac{\overline{P_{tr}}}{K}\right)^{-(Km_2+Km_3)} G_{2,2:0,1:1,2}^{2,1:1,0:1,1}\left(\begin{array}{c} {\scriptstyle -Km_2-Km_3,1-Km_2-Km_3} \\ {\scriptstyle -Km_2-Km_3,-Km_2-Km_3} \end{array} \left| \begin{array}{c} - \\ 0 \end{array} \right| \begin{array}{c} {\scriptstyle 1-Km_2} \\ {\scriptstyle 0,1-Km_2-Km_3} \end{array} \left| \tfrac{m_3 K}{\overline{\beta^2}\Omega\overline{P_{tr}}}, \tfrac{K\left(\frac{m_2}{\overline{\alpha^2}\Omega} - \frac{m_3}{\overline{\beta^2}\Omega}\right)}{\overline{P_{tr}}} \right.\right) \\ &-\varepsilon_t \log K \left(\tfrac{m_3}{\overline{\beta^2}\Omega}\right)^{-(Km_2+Km_3)} G_{2,2}^{1,2}\left(\begin{array}{c} 1-Km_2-Km_3, 1-Km_2 \\ 0, 1-Km_2-Km_3 \end{array} \left| \left(\tfrac{m_2}{\overline{\alpha^2}} - \tfrac{m_3}{\overline{\beta^2}}\right) \tfrac{\overline{\beta^2}}{m_3} \right.\right) \end{aligned}, \tag{24a}$$

$$\varepsilon_t = \left(\frac{m_2}{\overline{\alpha^2}\Omega}\right)^{Km_2} \left(\frac{m_3}{\overline{\beta^2}\Omega}\right)^{Km_3} \frac{1}{\Gamma\left(Km_2\right)}. \tag{24b}$$

rate per cell increases with the increase of the user number in a cell. This result indicates that the maximum achievable rate is mainly affected by the channel fading in the low interference case, i.e., the inter-cell power interference factor is less than 0.67. In this case, the multi-user diversity gain can be implemented owing to fluctuations of fading channels. When the inter-cell signal interference factor is large than or equal to 0.67, the maximum achievable rate per cell decreases with the increase of the user number in a cell. This result implies that the maximum achievable rate is mainly affected by the interference in the high interference case, i.e., the inter-cell power interference factor is large than or equal to 0.67. Moreover, the interfering users in adjacent cells will increase if the number of users per cell is increased. In this case, the maximum achievable rate decreases with the increasing number of users in the high interference region. This result is consistent with the result in interference-limited cellular networks [39].

V. Maximum Achievable Rate with Location Dependent Inter-cell Signal Interference Factors

In all aforementioned maximum achievable rate studies, users are assumed to be uniform and i.i.d. and with a random movement that preserves the uniform spatial distribution. In this case, the user's random motion cannot change the statistical characteristics of user distribution in a cell. Therefore, the inter-cell signal interference factor can be reasonably approximated by a constant. However, in some applications, such as interfering users in a running train, the movement of all interfering users in a cell has a specific and common direction. As a consequence, the inter-cell signal interference factor becomes time-varying and depends on the movement of users when computing the maximum achievable rate. In this section, a running train scenario is illustrated and then the maximum achievable rate with location dependent inter-cell signal interference factors for cellular networks with Nakagami-m fading uplink channels is presented.

A. A Running Train Scenario

Based on the generic system model in Fig. 1, a more detailed model for the specific running train scenario is illustrated in Fig. 6. The distance between the center of train and BS_{m-1} is r and the angle subtended by the center of train and BS_m at BS_{m-1} is θ. The length and width of train is assumed to be l and w, respectively. The train is assumed to be moving from BS_{m-1} to BS_m and all interfering users lie in the train. All users are assumed to be uniformly distributed in a train. To simplify the analysis, users in the m^{th} cell is assumed only be interfered by train users in the $(m-1)^{th}$ cell in this scenario, that is the interference signal just come from one side. The speed of train is assumed to be slow, such as less than 80 kilometers per hour, to avoid the Doppler frequency shift effect on uplinks of cellular networks.

B. Maximum Achievable Rate with Location Dependent Inter-cell Signal Interference Factor

Considering that all interfering users lie in a running train and move together, all interfering users in a train are assumed to have the same interference factor. In this case, the average inter-cell power interference factor is used for the same interference factor of all interfering users in a running train. Moreover, the average inter-cell power interference factor $\overline{\alpha^2}$ is expressed by

$$\overline{\alpha^2} = \frac{\int \alpha^2 ds}{S_{train}} = \frac{\int_{\theta-\frac{l}{2r}}^{\theta+\frac{l}{2r}} \int_{r-\frac{w}{2}}^{r+\frac{w}{2}} \alpha^2 q dq d\phi}{\int_{\theta-\frac{l}{2r}}^{\theta+\frac{l}{2r}} \int_{r-\frac{w}{2}}^{r+\frac{w}{2}} q dq d\phi}, \tag{25}$$

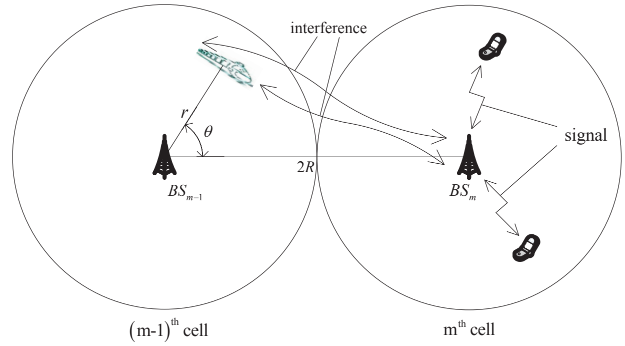

Fig. 6. A running train scenario.

where S_{train} is the train area and with a bit abuse of the term, we use the same symbol to denote the area of the train and the size of the area.

Based on the Cauchy-Schwarz inequality, the following result on a lower bound of total inter-cell power interference factor at the train can be obtained:

$$\begin{aligned}
&\int_{\theta-\frac{l}{2r}}^{\theta+\frac{l}{2r}} \int_{r-\frac{w}{2}}^{r+\frac{w}{2}} \alpha^2 q dq d\phi \\
&\geqslant \frac{\left(\int_{\theta-\frac{l}{2r}}^{\theta+\frac{l}{2r}} \int_{r-\frac{w}{2}}^{r+\frac{w}{2}} dq d\phi\right)^2}{\int_{\theta-\frac{l}{2r}}^{\theta+\frac{l}{2r}} \int_{r-\frac{w}{2}}^{r+\frac{w}{2}} \frac{1}{\alpha^2 q} dq d\phi} \\
&= \frac{(wl/r)^2}{\int_{\theta-\frac{l}{2r}}^{\theta+\frac{l}{2r}} \int_{r-\frac{w}{2}}^{r+\frac{w}{2}} \frac{1}{\alpha^2 q} dq d\phi} \\
&= \frac{(wl/r)^2}{\int_{\theta-\frac{l}{2r}}^{\theta+\frac{l}{2r}} \int_{r-\frac{w}{2}}^{r+\frac{w}{2}} \frac{\left(\sqrt{q^2-4Rq\cos\phi+4R^2}\right)^{\lambda}}{q^{\lambda+1}} dq d\phi}
\end{aligned} . \tag{26}$$

To simplify the derivation, the attenuation coefficient λ is fixed at 4 in the following computation, which corresponds to a typical urban macrocell environment [40]. Hence, (26) is further simplified as

$$\int \alpha^2 q dq d\phi \geq \frac{(wl/r)^2}{\delta - \eta + \zeta} \tag{27a}$$

with

$$\delta = \left(\ln\left(\frac{2r+w}{2r-w}\right) + \frac{16R^2 rw}{\left(r^2 - \frac{w^2}{4}\right)^2} + \frac{8R^4 rw\left(r^2 + \frac{w^2}{4}\right)}{\left(r^2 - \frac{w^2}{4}\right)^4} \right) \frac{l}{r}, \tag{27b}$$

$$\eta = \left(\frac{16Rw}{r^2 - \frac{w^2}{4}} + \frac{64R^3 w\left(3r^2 + \frac{w^2}{4}\right)}{3\left(r^2 - \frac{w^2}{4}\right)^3} \right) \cos\theta \sin\frac{l}{2r}, \tag{27c}$$

$$\zeta = \frac{8R^2 rw}{\left(r^2 - \frac{w^2}{4}\right)^2} \cos 2\theta \sin\frac{l}{r}. \tag{27d}$$

Substitute (27a) into (25), a lower bound of the average inter-cell power interference factor is obtained.

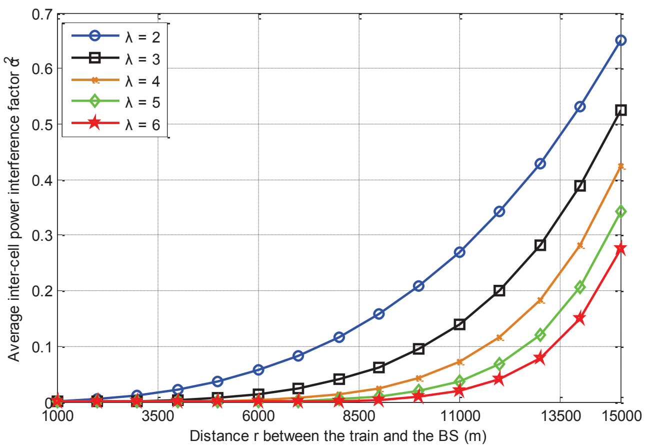

Fig. 7. Average inter-cell power interference factor with respect to the path loss exponent λ and the distance r between the train and the BS.

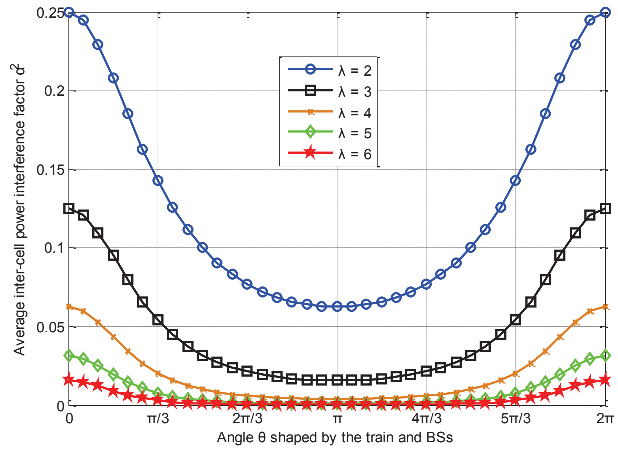

Fig. 8. Average inter-cell power interference factor with respect to the angle θ shaped by the train and BSs.

$$\overline{\alpha^2} \geq \frac{wl/r^2}{\delta - \eta + \zeta}. \tag{28}$$

Furthermore, considering that the interference just lies in one side cell, the inter-cell average power interference factor $\overline{\beta^2}$ in (13) is configured as zero. From (13), the maximum achievable rate with Nakagami-m fading uplink channels for the special case of a running train scenario can be rewritten as (29a) with (29b) and (29c).

Substitute (28) into (29a), an upper bound of the maximum achievable rate with location dependent inter-cell signal interference factors is given by (30).

C. Numerical Results and Discussion

Based on the proposed running train scenario in Fig. 6, the effect of wireless channel conditions and the train location on the average inter-cell power interference factor and the maximum achievable rate is investigated. In the following numerical results, the parameters are configured as follows: the length and width of train are configured as $l = 500$ and $w = 3.1$ meters [41]; the radius of cell is given by $R = 15000$ meters [42]; the Nakagami-m fading severity parameters are configured as $m_1 = m_2 = 2$; the number of users in a cell is configured as $K = 100$.

Fig. 7 illustrates the average inter-cell power interference factor with respect to the attenuation coefficient λ and the distance r between the train and the BS BS_{m-1}. Without loss of generality, the angle θ is chosen to be $\theta = {}^{\pi}/_{6}$ in Fig. 7. It is shown that the average inter-cell power interference factor increases with the increase of the distance between the train and the BS BS_{m-1}. When the distance between the train and the BS BS_{m-1} is fixed, the average inter-cell power interference factor decreases with the increase of the attenuation coefficient.

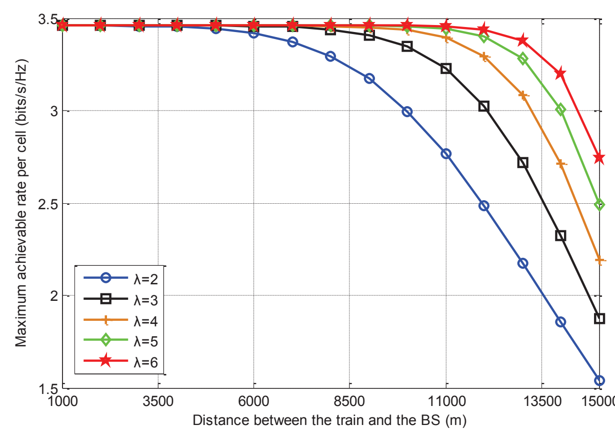

Fig. 9. Maximum achievable rate with respect to the path loss exponent λ and the distance r between the train and the BS.

In Fig. 8, the effect of the angle θ on the average inter-cell power interference factor is investigated. The distance between the train and the BS is fixed at $r = 10000$ meters in Fig. 8. As shown in Fig. 8, the average inter-cell power interference factor decreases when θ increases from 0 to π. However, the average inter-cell power interference factor increases when θ increases from π to 2π. The minimum of the average inter-cell power interference factor is reached when θ equals to π. When θ equals to 0 or 2π, the average inter-cell power interference factor reaches its maximum.

Fig. 9 shows the maximum achievable rate with respect to the attenuation coefficient and the distance r. Without loss of generality, the angle θ is configured as $\theta = {}^{\pi}/_{6}$ in Fig. 9. The maximum achievable rate decreases with the increasing of the distance between the train and the BS BS_{m-1}. When

$$\begin{aligned} R_{SCP\_m} &= \frac{1}{\varepsilon_1}\int_0^\infty \log\left(K+\bar{P}_t x\right) x^{Km_1+Km_2-1} e^{-m_2 x/\overline{\alpha^2}\Omega} {}_1F_1\left[Km_1; Km_1+Km_2; \left(\frac{m_2}{\overline{\alpha^2}\Omega}-\frac{m_1}{\Omega}\right)x\right] dx \\ &- \frac{1}{\varepsilon_2}\int_0^\infty \log\left(K+\bar{P}_t x\right) x^{Km_2-1} e^{\left(-\frac{m_2}{\overline{\alpha^2}\Omega}x\right)} dx \end{aligned} \tag{29a}$$

$$\varepsilon_1 = \left(\frac{\Omega}{m_1}\right)^{Km_1}\left(\frac{\overline{\alpha^2}\Omega}{m_2}\right)^{Km_2}\Gamma\left(Km_1+Km_2\right), \tag{29b}$$

$$\varepsilon_2 = \left(\frac{\overline{\alpha^2}\Omega}{m_2}\right)^{Km_2}\Gamma\left(Km_2\right). \tag{29c}$$

$$R_{SCP\_m} = \varepsilon_o\left(\frac{\overline{P_t}}{K}\right)^{-Km_1-Km_2} G_1 + \varepsilon_o \log K\left(\frac{m_2}{\overline{\alpha^2}\Omega}\right)^{-Km_1-Km_2} G_2 - \frac{1}{\Gamma\left(Km_2\right)} G_3 - \log K, \tag{30a}$$

$$\varepsilon_o = \left(\frac{m_1}{\Omega}\right)^{Km_1}\left(\frac{m_2}{\overline{\alpha^2}\Omega}\right)^{Km_2}\frac{1}{\Gamma\left(Km_1\right)}, \tag{30b}$$

$$G_1 = G^{2,1:1,0:1,1}_{2,2:0,1:1,2}\left(\begin{matrix} -Km_1-Km_2, 1-Km_1-Km_2 \\ -Km_1-Km_2, -Km_1-Km_2 \end{matrix}\middle| \begin{matrix} - \\ 0 \end{matrix} \middle| \begin{matrix} 1-Km_1 \\ 0, 1-Km_1-Km_2 \end{matrix}\middle| \frac{m_2 K}{\overline{\alpha^2}\Omega\overline{P_t}}, \frac{K\left(\frac{m_1}{\Omega}-\frac{m_2}{\overline{\alpha^2}\Omega}\right)}{\overline{P_t}}\right), \tag{30c}$$

$$G_2 = G^{1,2}_{2,2}\left(\begin{matrix} 1-Km_1-Km_2, 1-Km_1 \\ 0, 1-Km_1-Km_2 \end{matrix}\middle| \left(\frac{m_1}{\Omega}-\frac{m_2}{\overline{\alpha^2}\Omega}\right)\frac{\overline{\alpha^2}\Omega}{m_2}\right), \tag{30d}$$

$$G_3 = G^{1,3}_{3,2}\left(\begin{matrix} 1-Km_2, 1, 1 \\ 1, 0 \end{matrix}\middle| \frac{\overline{P_t}\overline{\alpha^2}\Omega}{Km_2}\right), \tag{30e}$$

$$\overline{\alpha^2} = \frac{wl/r^2}{\delta-\eta+\zeta}, \tag{30f}$$

$$\delta = \left(\ln\left(\frac{2r+w}{2r-w}\right) + \frac{16R^2 rw}{\left(r^2-\frac{w^2}{4}\right)^2} + \frac{8R^4 rw\left(r^2+\frac{w^2}{4}\right)}{\left(r^2-\frac{w^2}{4}\right)^4}\right)\frac{l}{r}, \tag{30g}$$

$$\eta = \left(\frac{16Rw}{r^2-\frac{w^2}{4}} + \frac{64R^3 w\left(3r^2+\frac{w^2}{4}\right)}{3\left(r^2-\frac{w^2}{4}\right)^3}\right)\cos\theta\sin\frac{l}{2r}, \tag{30h}$$

$$\zeta = \frac{8R^2 rw}{\left(r^2-\frac{w^2}{4}\right)^2}\cos 2\theta\sin\frac{l}{r}. \tag{30i}$$

$$\frac{2\gamma^2 R\cos\theta + 2\gamma R\sqrt{1-\gamma^2\sin^2\theta}}{\left(\gamma^2-1\right)} \le r \le \frac{2\gamma^2 R\cos\theta - 2\gamma R\sqrt{1-\gamma^2\sin^2\theta}}{\left(\gamma^2-1\right)}. \tag{33}$$

the distance between the train and the BS BS_{m-1} is fixed, the maximum achievable rate increases with the increase of the attenuation coefficient.

Fig. 10 evaluates the impact of θ on the maximum

$$\begin{cases} 0 \leqslant r \leqslant R & \frac{1}{3} < \gamma \leqslant 1 \quad and \quad \arccos\frac{5\gamma^2-1}{4\gamma^2} \leqslant \theta \leqslant \pi \\ 0 \leqslant r \leqslant \dfrac{2\gamma^2 R\cos\theta - 2\gamma R\sqrt{1-\gamma^2\sin^2\theta}}{(\gamma^2-1)} & others \end{cases} . \tag{35}$$

$$\begin{aligned} F_{\mathcal{G}}(\gamma) &= \iint\limits_{\frac{r}{\sqrt{(r\cos\theta-2R)^2+r^2\sin^2\theta}} \leqslant \gamma} \frac{r}{\pi R^2} dr d\theta \\ &= \int_0^{\pi} \int_0^{\frac{2\gamma^2 R\cos\theta - 2\gamma R\sqrt{1-\gamma^2\sin^2\theta}}{(\gamma^2-1)}} \frac{2r}{\pi R^2} dr d\theta \\ &= \frac{1}{\pi R^2(\gamma^2-1)^2} \int_0^{\pi} \left(2\gamma^2 R\cos\theta - 2\gamma R\sqrt{1-\gamma^2\sin^2\theta}\right)^2 d\theta \\ &= \frac{4\gamma^2}{(\gamma^2-1)^2} \end{aligned} . \tag{36}$$

$$\begin{aligned} F_{\mathcal{G}}(\gamma) &= \iint\limits_{\frac{r}{\sqrt{(r\cos\theta-2R)^2+r^2\sin^2\theta}} \leqslant \gamma} \frac{r}{\pi R^2} dr d\theta \\ &= \int_0^{\arccos\frac{5\gamma^2-1}{4\gamma^2}} \int_0^{\frac{2\gamma^2 R\cos\theta - 2\gamma R\sqrt{1-\gamma^2\sin^2\theta}}{(\gamma^2-1)}} \frac{2r}{\pi R^2} dr d\theta + \int_{\arccos\frac{5\gamma^2-1}{4\gamma^2}}^{\pi} \int_0^{R} \frac{2r}{\pi R^2} dr d\theta \\ &= \frac{1}{\pi R^2(\gamma^2-1)^2} \int_0^{\arccos\frac{5\gamma^2-1}{4\gamma^2}} \left(2\gamma^2 R\cos\theta - 2\gamma R\sqrt{1-\gamma^2\sin^2\theta}\right)^2 d\theta + \int_{\arccos\frac{5\gamma^2-1}{4\gamma^2}}^{\pi} \frac{1}{\pi} d\theta \\ &= 1 - \frac{(\gamma^2+1)^2 \arccos\frac{5\gamma^2-1}{4\gamma^2}}{\pi(\gamma^2-1)^2} - \frac{\sqrt{(9\gamma^2-1)}(1-\gamma^2)^{-\frac{1}{2}}}{2\pi} - \frac{4\gamma^2}{\pi(\gamma^2-1)^2} \arcsin\frac{\sqrt{(1-9\gamma^2)(\gamma^2-1)}}{4\gamma} \end{aligned} . \tag{37}$$

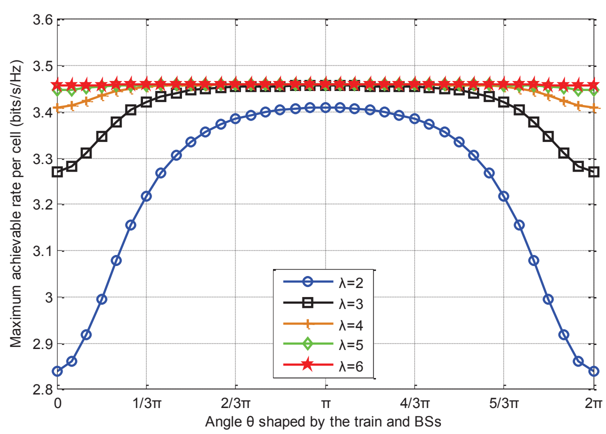

Fig. 10. Maximum achievable rate with respect to the angle θ shaped by the train and BSs.

achievable rate. The distance of the train and the BS is fixed at $r = 10000$ meters in Fig. 10. As shown in Fig. 10, the maximum achievable rate increases when θ increases from 0 to π. Moreover, the maximum achievable rate is decreased when θ increases from π to 2π. When θ equals to π, the maximum achievable rate reaches the upper limit. When θ equals to 0 or 2π, the maximum achievable rate reaches the lower limit.

VI. Conclusions

In this paper, the PDF of inter-cell power interference factor for linear Wyner cellular networks has been derived considering a realistic spatial distribution of user locations. The closed form result of the maximum achievable rate in cellular uplink channels has also been derived under the Nakagami-m fading model. Based on these, an upper bound of the maximum achievable rate with location dependent inter-cell signal interference factors is calculated and analyzed for a running train scenario. The PDF of the inter-cell power interference factor can be used to evaluate the interference power depending on the locations of users. Moreover, results of the maximum achievable rate for the running train scenario can provide useful guidelines for the deployment of BSs along the railways.

Appendix

Derivation of (10)

Based on the integral condition of (9), i.e., $\frac{r}{\sqrt{(r\cos\theta-2R)^2+r^2\sin^2\theta}} \leq \gamma$, we derive the following result by

$$\left(\gamma^2 - 1\right) r^2 - 4\gamma^2 Rr\cos\theta + 4\gamma^2 R^2 \geq 0. \qquad (31)$$

Considering the relationship of $\alpha^2 = \mathcal{G}^{\lambda}$, the range of γ is configured as $0 \leq \gamma \leq 1$. Moreover, a quadratic function $\Phi(r)$ is set as

$$\Phi(r) = \left(\gamma^2 - 1\right) r^2 - 4\gamma^2 Rr\cos\theta + 4\gamma^2 R^2. \qquad (32)$$

The graph of $\Phi(r)$ is an opening downward parabola with the maximum limit of $\frac{4\gamma^2 R^2\left(\gamma^2\sin^2\theta - 1\right)}{\gamma^2 - 1}$.

Based on (31) and properties of quadratic functions, the range of r is expressed as (33). Considering r is the distance between the specified user and the BS, the range of r is constrained by

$$0 < r \leq R. \qquad (34)$$

Considering the symmetry of the user's location, we just discuss the scenario where the user lies in the region with $\theta \in [0, \pi]$. The same result is used in the scenario where the user lies in the region with $\theta \in (\pi, 2\pi)$. Based on (33) and (34), the piecewise function is derived by (35).

When $0 \leq \gamma \leq \frac{1}{3}$, the CDF of $\mathcal{G}$ is derived as (36). When $\frac{1}{3} < \gamma \leq 1$, the CDF of $\mathcal{G}$ is derived as (37).

Combined with (36) and (37), the result of (10) is derived.

References

[1] H. Zhu, "On frequency reuse in cooperative distributed antenna systems," *IEEE Commun. Mag.*, vol. 50, no. 4, pp. 85–89, April 2012.

[2] W. W. L. Ho, T. Q. S. Quek, S. Sun and R. W. Heath, "Decentralized Precoding for Multicell MIMO Downlink," *IEEE Trans. Wireless Commun.*, vol.10, no.6, pp. 1798–1809, June 2011.

[3] J. Lee, S. Bae, Y. Kwon and M. Chung, "Interference Analysis for Femtocell Deployment in OFDMA Systems Based on Fractional Frequency Reuse," *IEEE Commun. Lett.*, vol. 15, no. 4, pp. 425–427, April 2011.

[4] D. Gesbert, S. Hanly, H. Huang, S. S. Shitz, O. Simeone and Y. Wei, "Multi-Cell MIMO Cooperative Networks: A New Look at Interference," *IEEE J. Sel. Areas Commun.*, vol. 28, no. 9, pp. 1380–1408, Dec. 2010.

[5] Y. Liang, T. Yoo, and A. Goldsmith, "Coverage Spectral Efficiency of Cellular Systems with Cooperative Base Stations," in *Proc. IEEE GLOBECOM*, Nov. 2006, pp. 1–5.

[6] Y. Liang and A. Goldsmith, "Adaptive Channel Reuse in Cellular Systems," in *Proc. IEEE ICC*, June 2007, pp. 857–862.

[7] J. Xu, J. Zhang, and J. G. Andrews, "On the Accuracy of the Wyner Model in Cellular Networks," *IEEE Trans. Wireless Commun.*, vol. 10, no. 9, pp. 3098–3109, Sep. 2011.

[8] H. J. Bang, D. Gesbert, and P. Orten, "On the Rate Gap Between Multi- and Single-Cell Processing Under Opportunistic Scheduling," *IEEE Trans. Signal Process.*, vol. 60, no. 1, pp. 415–425, Jan. 2012.

[9] S. V. Hanly and P. A. Whiting, "Information-theoretic capacity of multi-receiver networks," *Telecommun. Systems*, vol. 1, no. 1, pp. 1–42, Mar. 1993.

[10] A. D. Wyner, "Shannon-theoretic approach to a Gaussian cellular multiple-access channel," *IEEE Trans. Inform. Theory*, vol. 40, no. 6, pp. 1713–1727, Nov. 1994.

[11] S. Shamai and A. Wyner, "Information-theoretic considerations for symmetric, cellular, multiple-access fading channels. I," *IEEE Trans. Inform. Theory*, vol. 43, no. 6, pp. 1877–1894, Nov. 1997.

[12] O. Somekh, B. Zaidel, and S. Shamai, "Sum rate characterization of joint multiple cell-site processing," *IEEE Trans. Inform. Theory*, vol. 53, no. 12, pp. 4473–4497, Dec. 2007.

[13] S. Jing, D. N. C. Tse, J. B. Soriaga, J. Hou, J. E. Smee, and R. Padovani, "Downlink macro-diversity in cellular networks," in *Proc. IEEE ISIT*, June 2007, pp. 1–5.

[14] O. Somekh and S. Shamai, "Shannon-theoretic approach to a Gaussian cellular multiple-access channel with fading," *IEEE Trans. Inform. Theory*, vol. 46, no. 4, pp. 1401–1425, July 2000.

[15] N. Levy, O. Zeitouni, and S. Shamai, "Central limit theorem and large deviations of the fading Wyner cellular model via product of random matrices theory," *Problems of Inform. Trans.*, vol. 45, no. 1, pp. 5–22, Jan. 2009.

[16] N. Levy, O. Zeitouni, and S. Shamai, "On information rates of the fading Wyner cellular model via the thouless formula for the strip," *IEEE Trans. Inform. Theory*, vol. 56, no. 11, pp. 5495–5514, Nov. 2010.

[17] M. Bacha, J. Evans, and S. Hanly, "On the capacity of cellular networks with MIMO links," in *Proc. IEEE ICC*, June 2006, vol. 3, pp. 1337–1342.

[18] A. Sanderovich, O. Somekh, H. Vincent Poor and S. Shamai (Shitz), "Uplink macro diversity of limited backhaul cellular network," *IEEE Trans. Inform. Theory*, vol. 55, no. 8, pp. 3457–3478, Aug. 2009.

[19] B. Nazer, A. Sanderovich, M. Gastpar, and S. Shamai, "Structured superposition for backhaul constrained cellular uplink," in *Proc. IEEE ISIT*, June 2009, pp. 1530–1534.

[20] S. Shamai and B. Zaidel, "Enhancing the cellular downlink capacity via co-processing at the transmitting end," in *Proc. IEEE VTC-Spring*, May 2001, vol. 3, pp. 1745–1749.

[21] O. Simeone, O. Somekh, H. V. Poor, and S. Shamai, "Downlink multicell processing with limited backhaul capacity," *EURASIP J. Advan. Signal Process*, vol. 2009, 2009.

[22] X. Ge, K. Huang, C.-X. Wang, X. Hong, and X. Yang, "Capacity analysis of a multi-cell multi-antenna cooperative cellular network with co-channel interference," *IEEE Trans. Wireless Commun.*, vol. 10, no. 10, pp. 3298–3309, Oct. 2011.

[23] O. Somekh, O. Simeone, Y. Bar-Ness, A. Haimovich, and S. Shamai, "Cooperative multicell zero-forcing beamforming in cellular downlink channels," *IEEE Trans. Inform. Theory*, vol. 55, no. 7, pp. 3206–3219, July 2009.

[24] K. Huang, V. K. Lau, and Y. Chen, "Spectrum Sharing between Cellular and Mobile Ad Hoc Networks: Transmission-Capacity Trade-Off," *IEEE J. Sel. Areas Commun.*, vol. 27, no. 7, pp. 1256–1267, Sept. 2009.

[25] M. Grossglauser and D.N.C. Tse, "Mobility increases the capacity of ad hoc wireless networks," *IEEE Trans. Networking*, vol. 10, no. 4, pp. 477–486, Aug. 2002.

[26] A. Goldsmith, *Wireless Communications*. Cambridge, UK: Cambridge Univ. Press, 2005.

[27] M. Kobayashi and G. Caire, "Joint beamforming and scheduling for a multi-antenna downlink with imperfect transmitter channle knowledge," *IEEE J. Sel. Areas Commun.*, vol. 25, no. 7, pp. 1468–1477, Sept. 2007.

[28] C. Bettstetter, H. Hartenstein and X. Perez-Costa, "Stochastic Properties of the Random Waypoint Mobility Model: Epoch Length, Direction Distribution, and Cell Change Rate," in *Proc. ACM MSWiM*, Sept. 2002, pp. 7–14.

[29] A. Baddeley, "Spatial Point Processes and Their Applications," in *Stochastic Geometry: Lecture Notes in Mathematics*, Springer-Verlag Berlin Heidelberg, 2007.

[30] V.Erceg, L.J. Greenstein, S.Y. Tjandra, S.R. Parkoff, A.Gupta, B.Kulic, A.A. Julius, and R.Bianchi, "An empirically based path loss model for wireless channels in suburban environments," *IEEE J. Sel. Areas Commun.*, vol. 10, no. 5, pp. 1205–1211, July 1999.

[31] J. Wu, N .B Mehta, A. F. Molisch and J. Zhang, "Spectral eficiency of channel-aware scheduler in non-identical composite links with interference," in *Proc. ICC*, June 2007, pp. 5218–5223.

[32] P. S. Bithas, N. C. Sagias, P.T. Mathiopoulos, G.K. Karagiannidis, and A. A. Rontogiannis, "On the performance analysis of digital communications over generalized-K fading channels," *IEEE Commun. Lett.*, vol. 10, no. 5, pp. 353–355, May 2006.

[33] wikipedia. (2012) [Online]. Available: http://en.wikipedia.org/wiki/Gamma_distribution

[34] T. Pham-Gia and N. Turkkan, "System availability in a gamma alternating renewal process," *Naval Resear. Logist.*, vol. 46, pp. 832–844, Oct. 1999.

[35] I. S. Gradshteyn and I. M. Ryzhik, *Table of Integrals, Series, and Products*, 5th ed. New York: Academic Press, 2007.

[36] S. B. Provost, "On sums of independent gamma random variables," *Statistics*, no. 20, pp. 583-591, 1989.

[37] J. R. W. Health, W. Tao, K. Y. Hoon and C. K. S. Anthony, "Multiuser MIMO in Distributed Antenna Systems with Out-of-Cell Interference," *IEEE Trans. Signal Process.*, vol. 59, no. 10, pp. 4885–4899, Oct. 2011.

[38] Wolfram Mathworld. (2010) [Online]. Available: http://functions.wolfram.com/HypergeometricFunctions

[39] S. H. Kim, B. C. Jung, and D. K. Sung, “Effect of other-cell interference on multiuser diversity in cellular networks,” in *Proc. IEEE ISCIT*, Sept. 2007, pp. 521–525.

[40] 3GPP, “Spatial Channel Model for Multiple Input Multiple Output (MIMO) Simulations,” TR 25.996 v8.0.0, Dec. 2008.

[41] J.H. White, *The American Railroad Passenger Car*. Maryland, USA: The Johns Hopkins University Press, 1978.

[42] D. Astely, E. Dahlman, A. Furuskar, Y. Jading, M. Lindstrom, and S. Parkvall, “LTE: the evolution of mobile broadband,” *IEEE Commun. Mag.*, vol. 47, no. 4, pp. 44–51, Apr. 2009.

Jing Zhang received his M.S. and Ph.D. degrees in Electronics and Information engineer department from the Huazhong University of Science and Technology (HUST) in 2002 and 2010, respectively. He is now an associate professor in HUST. He has done research in the areas of MIMO, CoMP, beamforming, and next generation mobile communications. His current research interests are cellular systems, green communications, channel estimation, system performance analysis.

Xiaohu Ge (M’09-SM’11) is currently a Professor with the Department of Electronics and Information Engineering at Huazhong University of Science and Technology (HUST), China. He received his PhD degree in Communication and Information Engineering from HUST in 2003. He has worked at HUST since Nov. 2005. Prior to that, he worked as a researcher at Ajou University (Korea) and Politecnico Di Torino (Italy) from Jan. 2004 to Oct. 2005. He was a visiting researcher at Heriot-Watt University, Edinburgh, UK from June to August 2010. His research interests are in the area of mobile communications, traffic modeling in wireless networks, green communications, and interference modeling in wireless communications. He has published about 60 papers in refereed journals and conference proceedings and has been granted about 15 patents in China. He received the Best Paper Awards from IEEE Globecom 2010. He is leading several projects funded by NSFC, China MOST, and industries. He is taking part in several international joint projects, such as the RCUK funded UK-China Science Bridges: R&D on (B)4G Wireless Mobile Communications and the EU FP7 funded project: Security, Services, Networking and Performance of Next Generation IP-based Multimedia Wireless Networks.

Dr. Ge is currently serving as an Associate Editor for *International Journal of Communication Systems (John Wiley & Sons)*, *IET Wireless Sensor Systems*, *KSII Transactions on Internet and Information Systems* and *Journal of Internet Technology*. Since 2005, he has been actively involved in the organisation of more than 10 international conferences, such as Executive Chair of IEEE GreenCom 2013 and Co-Chair of workshop of Green Communication of Cellular Networks at IEEE GreenCom 2010. He is a Senior Member of the IEEE, a Senior member of the Chinese Institute of Electronics, a Senior member of the China Institute of Communications, and a member of the NSFC and China MOST Peer Review College.

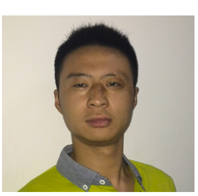

Zipeng Li received his Bachelor’s degree in telecommunication engineering from Huazhong University of Science and Technology (HUST) in June 2011. He is currently working toward his Master’s degree in communication and information systems at HUST. His research interests include inter-cell interference modeling and cooperative communication in cellular networks.

Guoqiang Mao received PhD in telecommunications engineering in 2002 from Edith Cowan University. He joined the School of Electrical and Information Engineering, the University of Sydney in December 2002 where he is an Associate Professor now. His research interest includes intelligent transport systems, applied graph theory and its applications in networking, wireless multihop networks, wireless localization techniques and network performance analysis. He is a Senior Member of IEEE and an Associate Editor of IEEE Transactions on Vehicular Technology.

Yang Yang is a member of the Founding Team for the School of Information Science and Technology at ShanghaiTech University, which is jointly established by the Shanghai Municipal Government and the Chinese Academy of Sciences (CAS). He currently holds a professorship at CAS Shanghai Institute of Microsystem and Information Technology and serves as the Director at Shanghai Research Center for Wireless Communications. Prior to that, he served the Department of Electronic and Electrical Engineering at University College London (UCL), United Kingdom, as a Senior Lecturer, the Department of Electronic and Computer Engineering at Brunel University, United Kingdom, as a Lecturer, and the Department of Information Engineering at The Chinese University of Hong Kong as an Assistant Professor.

Yang received the BEng and MEng degrees from Southeast University, P. R. China, in 1996 and 1999, respectively; and the PhD degree from the Chinese University of Hong Kong in 2002. His general research interests include wireless ad hoc and sensor networks, wireless mesh networks, next generation mobile cellular systems, intelligent transport systems, and wireless testbed development and practical experiments.